Available online at www.sciencedirect.com
SCIENCE DIRECT®
Sedimentary Geology 190 (2006) 269–287
Sedimentary Geology
www.elsevier.com/locate/sedgeo

Mesozoic climates: General circulation models and the rock record

Bruce W. Sellwood [a,*], Paul J. Valdes [b]

[a] Geosciences Building, School of Human and Environmental Sciences, The University, Whiteknights, Reading, RG6 6AB, UK
[b] School of Geographical Sciences, University of Bristol, University Road, Bristol, BS8 1SS, UK

Abstract

General circulation models (GCMs) use the laws of physics and an understanding of past geography to simulate climatic responses. They are objective in character. However, they tend to require powerful computers to handle vast numbers of calculations. Nevertheless, it is now possible to compare results from different GCMs for a range of times and over a wide range of parameterisations for the past, present and future (e.g. in terms of predictions of surface air temperature, surface moisture, precipitation, etc.). GCMs are currently producing simulated climate predictions for the Mesozoic, which compare favourably with the distributions of climatically sensitive facies (e.g. coals, evaporites and palaeosols). They can be used effectively in the prediction of oceanic upwelling sites and the distribution of petroleum source rocks and phosphorites. Models also produce evaluations of other parameters that do not leave a geological record (e.g. cloud cover, snow cover) and equivocal phenomena such as storminess. Parameterisation of sub-grid scale processes is the main weakness in GCMs (e.g. land surfaces, convection, cloud behaviour) and model output for continental interiors is still too cold in winter by comparison with palaeontological data. The sedimentary and palaeontological record provides an important way that GCMs may themselves be evaluated and this is important because the same GCMs are being used currently to predict possible changes in future climate.

The Mesozoic Earth was, by comparison with the present, an alien world, as we illustrate here by reference to late Triassic, late Jurassic and late Cretaceous simulations. Dense forests grew close to both poles but experienced months-long daylight in warm summers and months-long darkness in cold snowy winters. Ocean depths were warm (8 °C or more to the ocean floor) and reefs, with corals, grew 10° of latitude further north and south than at the present time. The whole Earth was warmer than now by 6 °C or more, giving more atmospheric humidity and a greatly enhanced hydrological cycle. Much of the rainfall was predominantly convective in character, often focused over the oceans and leaving major desert expanses on the continental areas. Polar ice sheets are unlikely to have been present because of the high summer temperatures achieved. The model indicates extensive sea ice in the nearly enclosed Arctic seaway through a large portion of the year during the late Cretaceous, and the possibility of sea ice in adjacent parts of the Midwest Seaway over North America. The Triassic world was a predominantly warm world, the model output for evaporation and precipitation conforming well with the known distributions of evaporites, calcretes and other climatically sensitive facies for that time.

The message from the geological record is clear. Through the Phanerozoic, Earth's climate has changed significantly, both on a variety of time scales and over a range of climatic states, usually baldly referred to as "greenhouse" and "icehouse", although these terms disguise more subtle states between these extremes. Any notion that the climate can remain constant for the convenience of one species of anthropoid is a delusion (although the recent rate of climatic change is exceptional).
© 2006 Elsevier B.V. All rights reserved.

Keywords: Climate models; Triassic; Jurassic; Cretaceous; Palaeoclimates

* Corresponding author.
E-mail address: b.w.sellwood@reading.ac.uk (B.W. Sellwood).

0037-0738/$ - see front matter © 2006 Elsevier B.V. All rights reserved.
doi:10.1016/j.sedgeo.2006.05.013

1. Introduction

Broad general documentations of the Earth's climate state through geological time, based largely on the evidence provided by climate proxy data (sedimentary facies, biota, geochemical information), have been made by many authors (e.g. Frakes, 1979; Crowley and North, 1991; Frakes et al., 1992; Parrish in Allen et al., 1994; Valdes et al., 1999; Huber et al., 2000; Skelton et al., 2003). Frakes (1979) suggested, on the basis of such data that, over the past 500 Ma, the earth has been generally warmer than at present. Two significant cool phases were indicated: the Permo-Carboniferous (Gondwana Glaciation) and the Quaternary to Holocene.

The predominance of episodes warmer than present ("greenhouse phases"), and relative rarity of intervals colder than present ("icehouse phases"), is particularly striking. Direct evidence for glaciation (from the distribution of facies such as tillites, ice-rafted dropstones, striated pavements, glendonites, etc.) outside of the Oligocene–Recent and Permo-Carboniferous, has led to the idea that equable conditions have prevailed in the past when, by implication, the earth is believed to have been generally ice-free. Based on negative evidence, the Mesozoic is believed by many to be such an ice-free time interval (e.g. Hallam, 1985, 1994). However, based on accumulating positive evidence, it has been recognised, over the past decade, that the onset and growth of significant glaciation in Antarctica took place over a time-frame far greater that was originally thought. This has been recognised in terms of the isotopic record in the oceans, recording a progressive and stepwise increase in the $\delta^{18}O$ content of the ocean waters (e.g. Zachos et al., 1992, 2002). Recently, Tripati et al. (2005) have suggested that Antarctic glaciation could have even started in the mid-Eocene. Shackleton and Kennett (1975) have calculated that the mean value for $\delta^{18}O$ of an "ice-free" ocean would have been a δ_w of −1.0 per mil SMOW (cf. 0 per mil SMOW today). There is now direct sedimentary evidence from the Antarctic area itself of iceberg dropstone activity since the late Eocene and of icecap advances and retreats since around the Oligocene (e.g. Billups and Schrag, 2002) with the East Antarctic ice sheet rapidly growing to about its present size at about 15 Ma (summarised in Hall et al., 2003).

Rocks of the Mesozoic era, a time interval sandwiched between two mass extinction events (Benton, 2003), have yet to provide unequivocal evidence of glacial processes. There is, on the other hand, a wealth of information reflecting global average temperatures throughout the Mesozoic around 6 to 9 °C warmer than the present. This includes thermophylic organisms, including reef and tropical carbonate belts that extended at least 10° of latitude poleward of their present distributions (Sellwood and Price in Huber and Watkins, 1992; Allen et al., 1994; DeConto et al., 2000, and review by Johnson et al., 2002), widespread bauxites and other palaeosols (Price et al., 1997), extensive distributions of evaporites and desert deposits, ocean-derived palaeotemperature data (Bice et al., 2003; Crowley and Zachos in Huber et al., 2000; Sellwood and Price, op. cit.) and information from temperature-sensitive terrestrial biota (e.g. Markwick, 1998; Spicer et al. in Allen et al., 1994). However, it should be cautioned that, recently, Pearson et al. (2001) have raised serious concerns about the interpretation of the isotope record. This warmth occurred despite the earth receiving, because of the sun's evolution, in the mid-Cretaceous around 1% less incident solar flux at the top of the atmosphere than it does today and at the start of the Jurassic almost 2% less.

Following a sea-level low at the start of the Triassic, and despite significant lowstands in the early Jurassic and in the early Cretaceous, it has been well established that global sea levels throughout much of the Mesozoic were generally much higher than at present. The apparent absence of major ice caps accounts for some of this eustatic rise (by comparison with the present), but absence of ice and the thermal expansion of water can only contribute around 100 m or so to the rise. In addition, high rates of sea floor spreading (on average 75% greater than at present) will have led, it is assumed, to the elevation of oceanic ridges and the displacement of ocean waters over what were, for most of the time interval, relatively subdued or subsident continental masses (e.g. Skelton et al., 2003).

A recent approach to understanding past climate regimes on Earth has been through the application of complex computer models, specifically: Atmospheric General Circulation Models (AGCMs), Ocean General Circulation Models (OGCMs) and recently with even more complex coupled ocean–atmosphere GCMs (OAGCM). There are now many contributions in this field with the following papers and reviews reflecting something of the evolution in this approach on both sides of the Atlantic: Barron (1983, 1987), Barron and Washington (1985), Kutzbach and Gallimore (1989), Chandler et al. (1992), Moore et al. (1992a,b), Valdes and Sellwood (1992), Barron et al. (1994), Kutzbach and Ziegler (1994), Price et al. (1995), Valdes et al. (1995), Handoh et al. (1999), Valdes et al. (1999), Poulsen et al. (2001) and Bjerrum et al. (2001).

Mesozoic greenhouse climates have even been considered as possible analogues for future climate (Crowley, 1996), thus heightening interest in model outputs on the Mesozoic.

We present here the output from new model simulations generated using the HadAM3 version of the UKMO atmosphere GCM, and we review geological data, and the output from other models, to throw light on the climate of the Mesozoic Earth and on the validity of the models themselves. The model simulations are based on atmosphere-only model but the results are similar to fully coupled model simulations which are currently underway.

2. Model description

The model was developed at the Hadley Centre for Climate Prediction and Research, which is part of the Meteorological Office. The GCM consists of a linked atmospheric model and sea ice model. The horizontal resolution of the atmospheric model is 2.5° in latitude and 3.75° in longitude. This provides a grid spacing at the equator of 278 km north to south and 417 km east to west. The atmospheric model consists of 19 layers. It also includes a radiation scheme that can represent the effects of minor trace gases. Its land surface scheme includes the representation of the freezing and melting of soil moisture. The representation of evaporation includes the dependence of stomatal resistance on temperature, vapour pressure and CO_2 concentration. There is an adiabatic diffusion scheme, to simulate the horizontal mixing of tracers.

Other aspects of the workings of this model have been described in Pope et al. (2000) and its use in palaeoclimate studies is illustrated in Haywood et al. (2002).

3. Triassic: model/proxy data comparison

For the Triassic, we present simulations from the atmospheric GCM, using a simple zonally symmetric sea surface temperature.

3.1. Temperatures (Fig. 1A and B)

A significant feature of the Triassic Earth is that landmasses are almost symmetrically distributed in a broad arc about the equator. A major aspect of the modelled earth is its overall warmth. Despite temperatures plunging to −20 °C and below over Siberia in northern hemisphere winter, and to similarly low values over southernmost Gondwana in southern hemisphere winter, the annual temperature average of the earth is subdued in these high-latitude areas because of the high summer values achieved there (~24 °C). These high summer values preclude the possibility of year-round ice and snow. Freezing temperatures are modelled to come on over Siberia during October, plunging to their lowest during February and then rapidly rising with the onset of Spring, in April. May to September are warm months with those regions experiencing the coldest winters achieving summer temperatures, which rise to the mid-20s. Continental regions between about 40°N and S are generally warm (>20 °C) throughout the year but have sustained highs into the 30s and 40s during most of the year. Air temperatures over the oceans are largely latitudinal and move, as expected, with the movement of the ITCZ.

3.2. Temperature-limited facies

From the model, low temperatures would not have been a significant inhibitor to coral reef development around the Tethys (Fig. 1A and B). According to Flügel (2002) after the set-back at the end-Permian mass extinction, reef systems developed and diversified through the Triassic, extending their range from between 2°S and 25°N in the mid-Triassic (Anisian) to a maximum range of 35°S to 33°N in the late Triassic (Norian). The Norian-Rhaetian sponge-coral and coral-dominated reefs are interpreted to have had ranges close to those of their modern counterparts. Range limits are very close to the 20 °C isotherm in the Upper Triassic model. Prolific reefs and associated platform carbonates are found throughout the Tethyan region, from Papua New Guinea, Timor, northern India, southern Europe, and along the northern margin to Thailand, Malaysia and Singapore (Flügel, 2002). On the Pacific (Panthalassa) margin of Pangaea coral reefs extend from Oregon in the north to northern Chile in the south. These localities lay close to the simulated 20 °C mean annual isotherm. Displaced terranes also exhibiting reefs (now in Japan and eastern Russia) may, according to Flügel (2002), have lain just north of 30°N, a scenario commensurate with modelled ocean temperatures. Central Pacific (Panthalassa) temperatures are generally simulated to be above 30 °C. This ocean is modelled as a having super, and semi-permanent, El Niño system. All Triassic reefs were affected by a global crisis at a time close to the Triassic–Jurassic boundary, disappearing from the western and southern Tethys and from Pacific microplates.

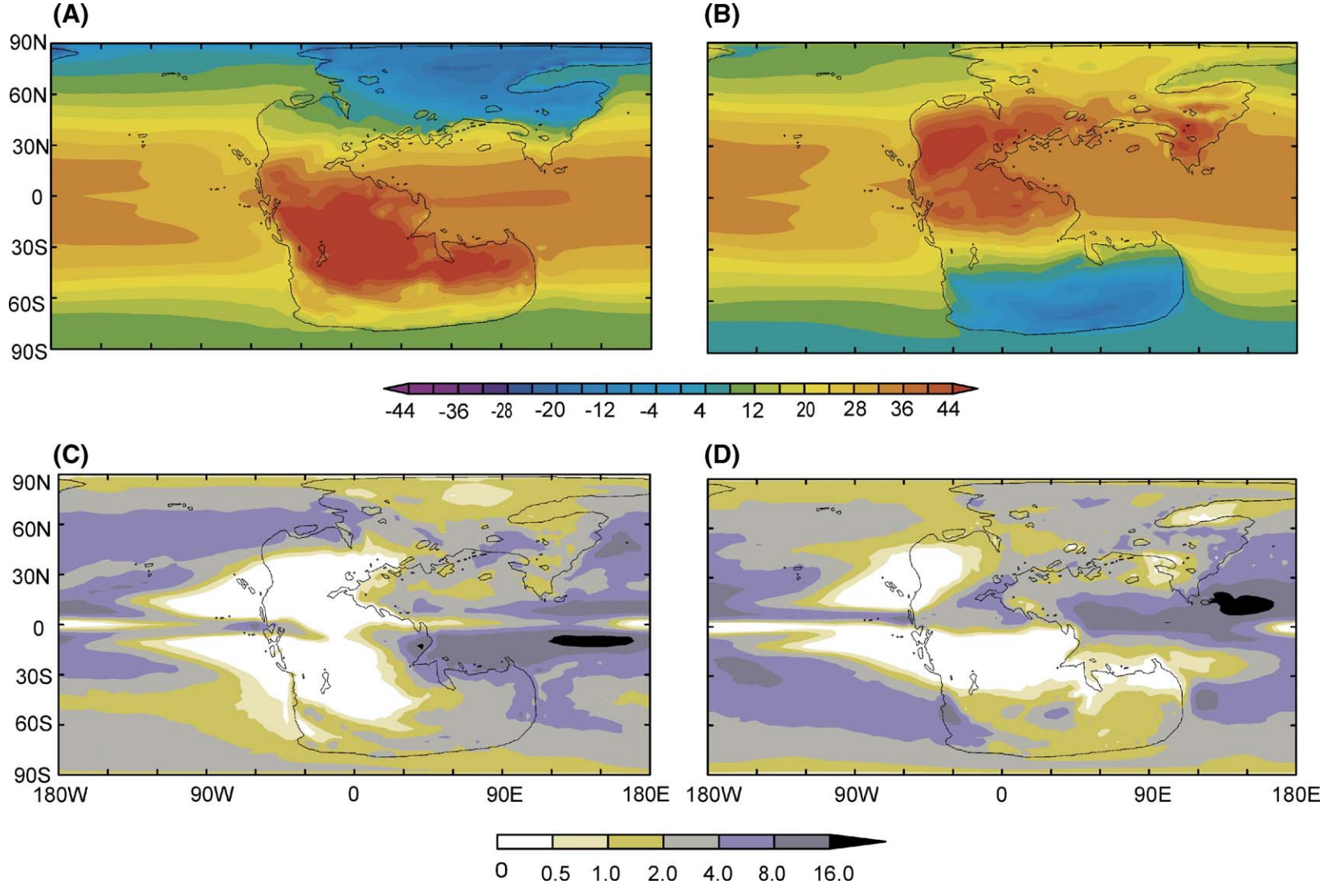

Fig. 1. (A and B) Model simulated mean seasonal temperatures for the Late Triassic, for (A) December–January–February season and (B) June–July–August season. Units are in °C and the contour interval is every 4 °C. The ocean sea surface temperatures were prescribed. (C and D) Model simulated, mean seasonal precipitation for the late Triassic, for (C) December–January–February season and (D) June–July–August season. Units are in mm/day and the contour interval is not regular.

3.3. Precipitation (Figs. 1C,D and 2A)

Large tracts of Pangaea between about 40°N and S are modelled to receive very little rainfall. Much of the planet's rainfall is over the oceans, being convective in character, with the main zone of rainfall migrating north and south through the year with the movement of the ITCZ. The equatorial lands surrounding eastern and southern Tethys are modelled to receive relatively little rainfall during the months of December through April with rains commencing in May, reaching a maximum in July, and then diminishing to virtually nothing through August to November. The Arabian–NE African part of Gondwana is modelled to have a monsoonal climate with major rains commencing in November, peaking in December through April, and evaporation exceeding

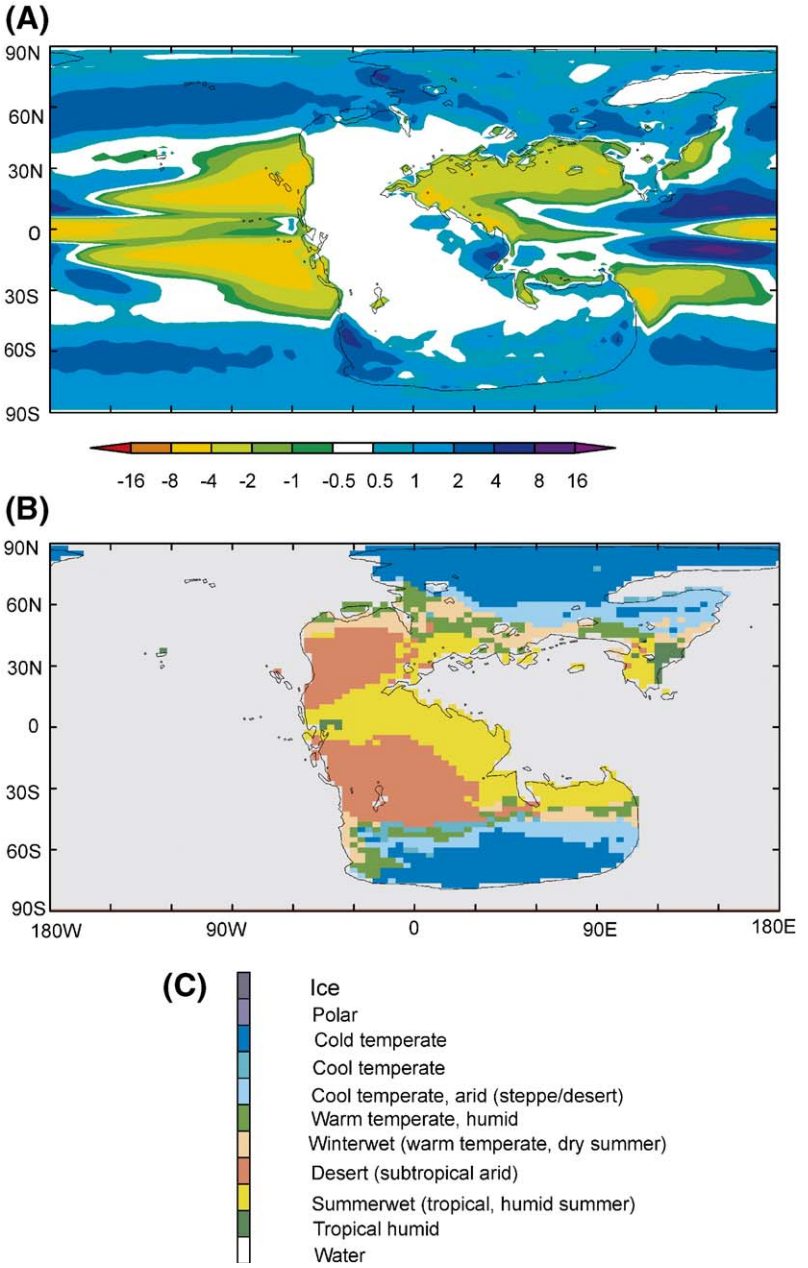

Fig. 2. (A) Modelled precipitation minus evaporation in mm/day for the Late Triassic (negative values indicate excess evaporation over precipitation). (B) The Walter biome zones for the Late Triassic based on the model predicted temperatures and precipitation. (C) Key to the Walter biome zones as used in subsequent figures.

precipitation for the rest of the year (winterwet, biome/climate zone 4 of Walter, 1985; Fig. 2A and B). Northern and eastern Siberia have some rainfall throughout the year, the wettest period being generally through June and the driest during the summer months of July and August, the period between April and September being either in balance with respect to evaporation and precipitation or with an excess of evaporation (equivalent to a winterwet biome 4 in the Walter scheme; Fig. 2A and B).

Southwestern Gondwana is also modelled to be winterwet. The eastern parts of Gondwana are moister than the western parts, being generally wetter during the summer months (particularly December, i.e. a modelled summerwet biome/climate zone 2; Fig 2B). The balance between evaporation and precipitation reflects these seasonal changes. Large tracts of Pangaea, particularly in the tropics, but extending to nearly 50°N and S, have a large excess of evaporation throughout much of the year, as does a large part of western Tethys. Southern Gondwana is either in balance, or has an excess of evaporation, from November through February (summer dryness). But from March through to October the southern parts of the continent in particular have an excess of precipitation (winterwet). This embraces the months of winter darkness for the southern polar area. Over the seaways, the relationship between evaporation and precipitation is expressed in ocean salinities raised above those of modern normal marine (35‰ NaCl), in particular the western end of the Tethys where precipitation minus evaporation is generally in excess of 2 mm/day (expressed as −2 mm on Fig. 2A). These values are modelled to give open sea salinities that exceed 40‰ and inshore values in excess of 45‰ NaCl.

3.4. Triassic facies and floras (Fig. 2C)

In the Triassic, the following climate zones of Walter (1985) have yet to be recognised from geological data: (10) ice, (9) polar, (8) cold temperate, (7) cold temperate arid (steppe/desert) (see also Scotese, 2000 Paleomap Project http://www.scotese.com). Tillites have not been reported (Frakes et al., 1992). An absence of both ice caps and these biomes would be expected from the model simulations.

According to Ziegler et al. (1994) in the early Triassic, the highest latitude floras contain the arborescent lycopod *Pleuromeia*, which has a world-wide distribution and reflects a global climate largely devoid of frosts, at least in coastal settings. From the global distribution of lithologic indicators of climate, Scotese (see above) considers the interior of Pangaea to have been hot and dry and notes that warm temperate climates extended to the poles. The Siberian flora was deciduous and displays well defined annual growth bands. These plants are interpreted to be equivalent to Walter's biome 6 (cool temperate) with cool winters and warm summers and a growing season of 4 to 8 months. The growing season would have started when daily temperatures reached 10 °C. From the model, N of 60° this would have been from mid-April to mid-October and S of 60° from late October to about mid-April. Growth would have continued as long as average precipitation was maintained at 20 mm/month, or more. According to the model, in neither Siberia nor southern Gondwana, is water availability likely to have been a limiting factor? To permit this biome to extend to 75° in both hemispheres, as is observed, would require poles far warmer than at present. This is consistent with modelled output. Scotese (2000) suggests that this may have been one of the hottest times in earth history, and the distribution of extensive calcretes throughout Europe and the western Tethyan margin is in agreement with the modelled climate: hot and predominantly arid but with a short wet season.

Relatively low diversity communities of microphyllous conifers (*Brachyphyllum*, *Pagiophyllum* and *Voltzaia*) were confined to lower latitudes, and are often found in the proximity of evaporites (usually found in both hemispheres between about 10° and 40° latitude). They thus represent the subtropical dry environment (biome 4) and their distributions are closely in line with model predictions in terms of the ratio between precipitation and evaporation.

Tropical coal disappears from the record in the early Triassic except for equatorial settings and Quingtang (China, then an isolated micro-continent at about 20°N, adjacent to Paleotethys).The coal facies have been interpreted as indicating a monsoonal climate, which is what is predicted by the model, with heavy rainfall from January through May. On the basis of facies and palaeobotanical data, warm temperate climates (biome 5) existed between 5° and the equator (Ziegler et al., 1994) with high diversity floras of ferns, cycads and seed ferns, as well as conifers and ginkgoes. The cool temperate zone is extended to central Siberia and is associated with postulated uplands of the Central Siberian Volcanic Traps.

During the Middle Trias, Europe had abundant evaporites and calcretes (see Scotese, 2000). In northern and southern China, warm temperate (biome 5) and cool temperate (biome 6) floras predominate (Ziegler et al., 1994). Again, this is fully in agreement with model output. Warm temperate floras (biome 5) extended to

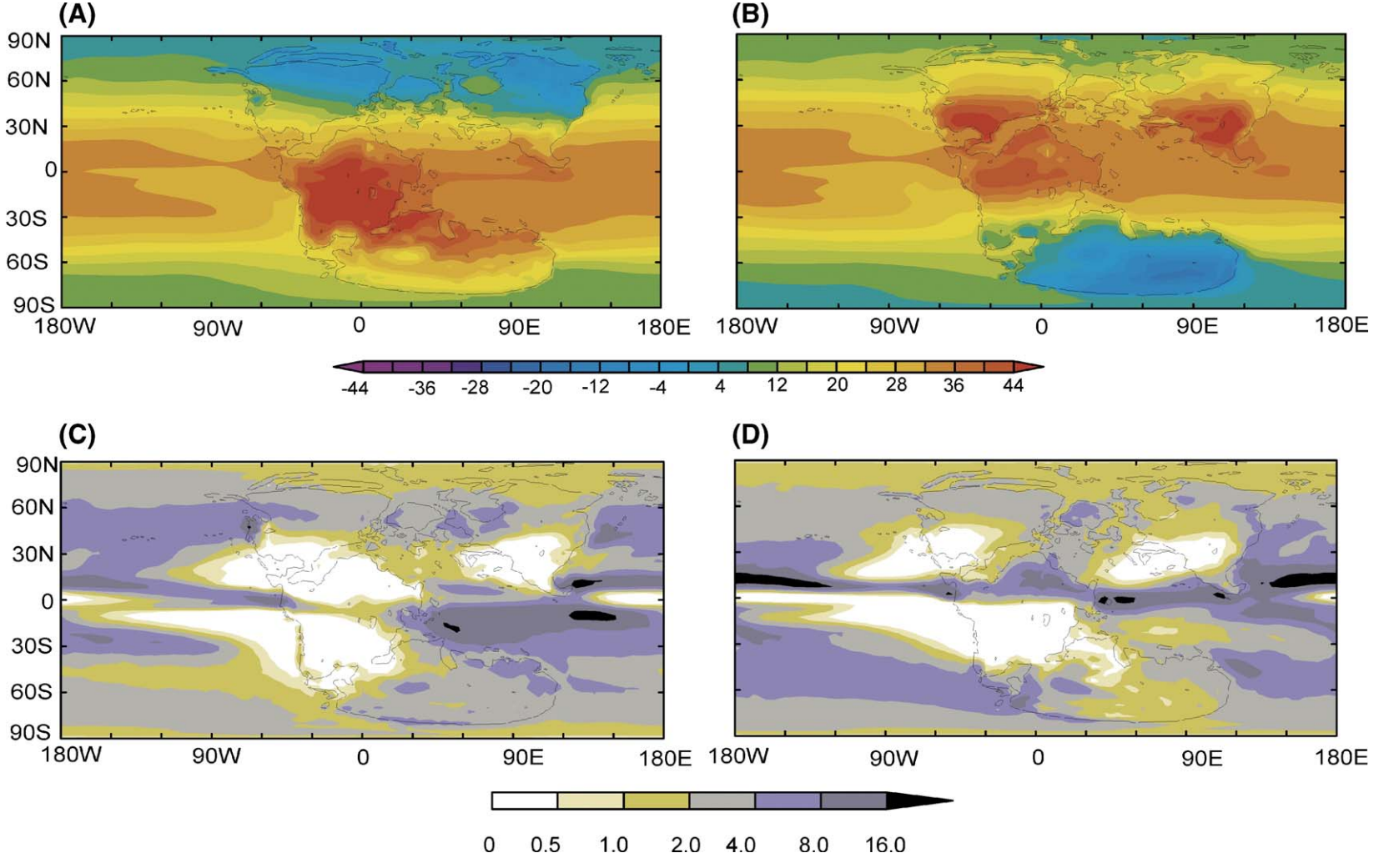

Fig. 3. (A and B) Model simulated mean seasonal temperatures for the Late Jurassic, for (A) December–January–February season and (B) June–July–August season. Units are in °C and the contour interval is every 4 °C. (C and D) Model simulated, mean seasonal precipitation for the Late Triassic, for (C) December–January–February season and (D) June–July–August season. Units are in mm/day and the contour interval is not regular.

about 70°N in northeastern Siberia and the first northern hemisphere coal swamps since the end-Permian mass extinction appear in this area. Southern hemisphere coal swamps are found in S Argentina, S Chile and Antarctica, again compatible with modelled zones with precipitation exceeding evaporation for much of the year. Biomes and facies suggest that the equatorial zone is a predominantly arid belt, again lending support to the validity of the model. Taylor and Taylor (2000) have studied exquisitely preserved fossil wood from the late Permian and middle Triassic of Victoria Land and the Transantarctic mountains. The sites, at 80–85°S in the Permian and 70–75°S in the Triassic, represent perimineralised peats, fluvial deposits and forests. Growth ring data suggests growth rates at these latitudes 1–2 orders of magnitude greater than today. The growth ring patterns suggest that the habitat was highly seasonal, with light, rather than temperature, being the limiting factor controlling plant growth and possibly reflecting long periods of winter darkness in these near polar habitats. Although some trees show evidence of frost damage (from an unseasonal frost early in the fall or late in the spring), the authors believe that the palaeobotanical evidence indicates that these areas were far warmer than predicted on the basis of either model or physical data alone.

It is interesting to note that Ziegler et al. (1984) suggested that light availability could have had an influence on the distribution of Mesozoic coral reefs whose distribution is less extensive than might have been expected by reference to other criteria.

In the late Trias, the warm temperate biome (biome 5) was dominant between 30° and 50° of latitude in both hemispheres. Floras typical of this biome are mixed with dry subtropical floras in the south, in S Europe, and with cool temperate floras to the N in northern China. There is not much in the way of climatic zonality and Meyen (1997) suspected that the whole earth may have been essentially frost-free. Ziegler et al. (1994) think this an overstated case. The model generally supports this scenario, but lack of precipitation typifies many continental interiors between these latitudes, especially away from the coastal zones.

Thus, the model output shows a good correlation with globally derived data, particularly that for terrestrial plant biomes and terrigenous proxy facies (Ziegler et al., 1994; Scotese, 2000), and also with the distribution of reefs (Flügel, 2002). Terrestrial reptile distributions (e.g. Tucker and Benton, 1984) are difficult to relate directly to palaeoclimate, but can be interpreted to be broadly in line with model output.

4. Jurassic (Kimmeridgian): model/proxy data comparison

4.1. Jurassic climate system (Figs. 3 and 4)

Late Jurassic models, largely based on Kimmeridgian or Tithonian times, are well described in the literature (reviewed in Valdes et al., 1999; Rees et al., 2000), so only the generalities of findings are reported here. For completeness, temperature, precipitation, precipitation–evaporation and biome outputs are presented as Figs. 3 and 4.

From fossil evidence, Jurassic plant productivity and maximum diversity were concentrated at mid-latitudes, reflecting a migration of the zone of peak productivity from low to higher latitudes during greenhouse times. Forests in mid-latitudes were dominated by a mixture of ferns, cycadophytes, sphenophytes, pteridophytes and conifers (reviewed and modelled in Rees et al., 2000). Low-latitude vegetation was predominantly xeromorphic and only patchily forested, with small-leafed forms of conifers and cycadophytes. Polar latitudes were dominated by broad-leafed conifers and ginkgophytes, which have been interpreted as deciduous. Tropical everwet (rainforest-type) biomes are rare or absent, as are tundra and glacial biomes. They recognise five main biomes: seasonally dry (summerwet), desert, seasonally dry (winterwet), warm temperate and cool temperate. The boundaries of these zones appear to have remained latitudinally fairly constant, the various continental masses moving through them as displacements occurred. There appear not to have been major global climatic changes throughout the period. Their compilation represents a considerable refinement on the approach of Hallam (1985, 1994), and the model simulations of Moore et al. (1992a,b), Valdes and Sellwood (1992), Valdes et al. (1995), Price et al. (1995) and references in these works. There is an apparently symmetrical arrangement of Jurassic coals and evaporites about the equator. This reflects evaporation/precipitation (rainfall) relationships with palaeolatitude. Broadly, the pattern suggests precipitation exceeded evaporation in mid- to high northern latitudes. Between about 30°N and the equator, evaporation is more than precipitation, whereas evaporation and precipitation are approximately in balance (E=P) around the equator. Between about 10° and 30°S, evaporation once again exceeds precipitation and, although evidence in the far south is sparse, there is a return to excess precipitation in the mid- to high southern latitudes. The patterns obtained from the

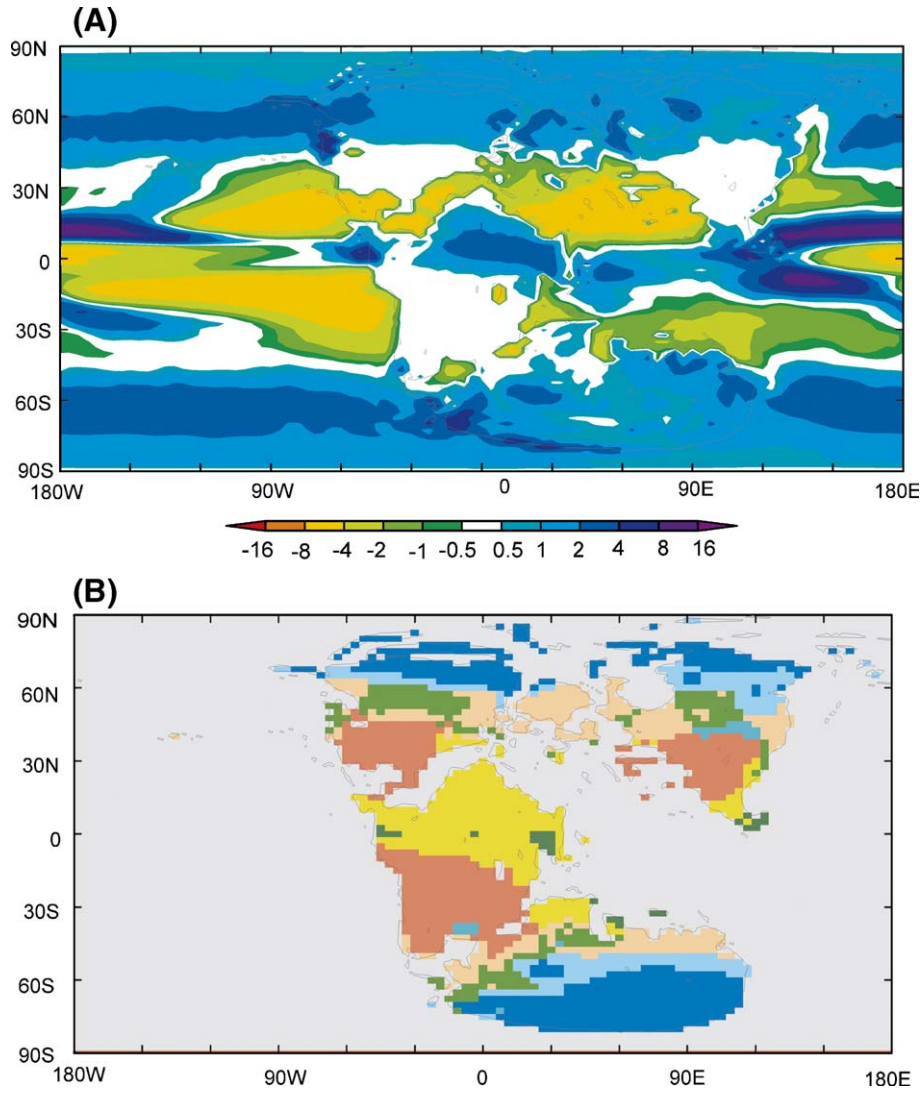

Fig. 4. (A) Modelled precipitation minus evaporation in mm/day for the Late Jurassic (negative values indicate excess evaporation over precipitation). (B) The Walter biome zones for the Late Jurassic based on the model predicted temperatures and precipitation. Key to zones as in Fig. 2C.

models are in broad agreement with the geological data presented and published previously (and reviewed in Valdes et al., 1999).

In the late Jurassic modelling described in Rees et al. (2000) and Valdes and Sellwood (1992), atmospheric CO_2 concentrations of four times present-day values were used. No major changes of climate are indicated for the Jurassic as a whole, and Rees et al. (2000) suspect that the climate zones they reported remained more-or-less constant but that because of plate movements continental areas moved across them. Such an interpretation requires support from palaeomagnetic data, which are, as yet, lacking. Hallam (1985), in an alternative hypothesis, suggested that the late Jurassic spread of aridity in S Eurasia was caused by regional tectonics, creating a rain shadow effect.

Marine invertebrate faunas in the Jurassic have long been recognised to be provincial rather than cosmopolitan in character, giving rise to the concept of so-called faunal realms. Two broad realms, largely based originally on ammonite distributions, are recognised, each associated with major geographical regions: Boreal (northern part of the northern hemisphere) and Tethyan (the rest of the world, but comprising a biota with much higher biodiversity than that of the Boreal Realm). Arkell (1956) originally proposed three realms. A third, the Pacific realm, was based on only a few distinctive ammonites in a fauna of predominantly Tethyan

character and so has subsequently been relegated to a province of the Tethyan realm (as reviewed in Hallam, 1975). Explanations of causes for these realms have ranged through: climatic (temperature and salinity), depth of sea, physical barriers and stress factors related to environmental stability.

Using the Princeton Ocean Model, Bjerrum et al. (2001) investigated potential water movements in the early Jurassic Laurasian Seaway that connected European Tethys with the Arctic Sea. The model suggested a north–south density difference, and hence a sea-level difference in the global ocean, which was the main factor forcing the seaway flow. When Tethys waters were denser than Arctic waters, then the net seaway flow was to the south. If Arctic waters were densest, then seaway flow was towards the north. They suggest that marine provincial boundaries were controlled by these density differences. Southward flowing currents, possibly related to oceanic thermohaline circulation, caused reduced-salinity Arctic waters to spread towards the Tethys, thus dispersing Boreal faunas southwards. The converse occurred during times of predominantly northerly flow. If this explanation is correct, it would imply a not unexpectedly complex interplay between climatic and the other factors in controlling provinciality.

The influence of a range of environmental factors, rather than temperature alone, in the generation of a possible palaeoclimate signal, is underlined by reference the Falkland area of the South Atlantic (Deep Sea Drilling Project Sites 330 and 511, Price and Sellwood, 1997). In this case apparently anomalously high seawater palaeotemperatures (17–18 °C at around palaeolatitude 60°S) derived from $\delta^{18}O$ values (−1.29‰ and −1.45‰ PDB) from belemnites. The marine shelf in this area was hemmed in by land areas and may have experienced enhanced fresh-water run-off, which might have depleted surface waters with respect to $\delta^{18}O$. So isotopic values need to be interpreted with caution, the "warmth" at these latitudes, being perhaps more apparent than real. A similar situation has recently also been reported from one of these sites (DSDP Site 511 for the Turonian Cretaceous, Bice et al., 2003).

5. Late Cretaceous: model/proxy data comparison

The model results shown are using the atmosphere model with prescribed sea surface temperatures which are based on provisional results from a fully coupled atmosphere–ocean (HadCM3L). These latter simulations have not reached complete equilibrium in the deep ocean and therefore we choose to show an atmosphere only simulation. However, we believe (based on evidence from previous work with this model) that the simulations are sufficiently close to the final coupled results and thus justify further analysis.

5.1. Modelled temperature (Fig. 5A and B)

During JJA, the model shows a very large proportion of eastern Asia (including much of China) to be a very hot area (>40 °C), with only the rising uplands in the extreme southeastern parts (Malaya/Indonesia) being slightly cooler. Mongolia and Siberia are warm (28 °C at 45°N) with 20 °C extending to the coast of the Arctic Sea. In June though July, cool temperatures (0–4 °C) persist over northernmost parts of the Arctic seaway. The scattered land areas of Eurasia (including Fennoscandia and Laurentia) that lay between 40°N and 80°N are generally above 20 °C and rise to more than 24 °C in July and August.

The large mid-west seaway over North America helps to ameliorate both summer and winter temperatures there, as had already been demonstrated by Valdes et al. (1996). Lowlands bordering the southern shores of this seaway are warm (>30 °C in July and August) and fall to around 20 °C in the far N (close to the Pole). The rising cordillera to the west of this seaway is a cool zone with temperatures below 12 °C, and this cool/mild zone continues northwards in a broad arc into what is now Alaska (generally12 °C+ rising to 20 °C+ in July). In the north, the onset of autumn occurs in mid-August, with temperatures beginning to fall everywhere north of the 60th parallel. The first frosts come in September, which sees the onset of sub-zero temperatures in Alaska–Beringia and the Arctic shore zones.

North Africa and northern South America are generally hot (>30 °C) rising to >36 °C just south of equator in June and remain hot (>36 °C) through July and August. A zone of steep temperature gradients occurs from around 30°S with temperatures falling to 16 °C and lower (locally approaching zero in South Africa in June and July). South America exhibits a similar pattern but not such low temperatures (Patagonia generally between 8 and 12 °C).

In June, the southern hemisphere island continent of India is mild everywhere and remains mild throughout the winter (12–20 °C). In the far north of India values of >20 °C occur throughout the winter. Another southern hemisphere island continent, Australia, is mild in the far north (12 °C rising towards 20 °C) but with cool (some sub-zero) temperatures in the far southeastern part, where temperatures remain low throughout July and

August (−4 °C and below). Antarctica generally has sub-zero values through the winter with lows below −20 °C over large parts of the continent in the mid-winter darkness.

In September and through October, eastern Asia (northern China and Siberia) suffer a rapid onset of autumn, with sub-zero temperatures spreading south of about 70°N. Southern China south of about 30°N remains warm at this time, with temperatures above 28 °C. Over the modelled uplands of SE Asia (Malaysia/Indonesia), slightly cooler values are recorded. A similar pattern extends westwards over the rest of the northern landmasses with sub-zero temperatures being the norm northeastwards of about 60°N from October onwards, and in the far north continental values fall as low as −30 °C during the dark month of January. There is a rapid transition southwards into mid-latitudes (approaching 30°N) where much milder conditions prevail (temperatures of around 8 °C and rising to 18 °C). Lands falling astride the equator remain hot to very hot throughout December, January and February (DJF) (generally >32 °C). The DJF hot belt extends southward to nearly 40°S.

Island India warms from October, high temperatures advancing southwards through November so, by December, most of the continent is at, or approaching, 30 °C and remains so through till February. March, April and May see gradual cooling to around 12 °C for most of the continent, except for the warmer far north.

During July, northern Australia, at around 30°S, experiences 12–20 °C, temperatures rapidly rising to >30 °C during January and February. Central and southern Australia achieve around 26 °C in January. In October, Antarctica has cool (near- and sub-zero values) over much of the continent but during November Antarctica generally thaws, although some areas are still sub-zero. However, much of the coastal strip achieves 4–12 °C. By December, all Antarctica is now very much above zero, with temperatures rising rapidly in the hinterland. Highland areas may still get late frosts, but the rest of the continent is >16 °C, and some areas are >24 °C, with continuous daylight promoting round-the-clock plant growth. There is cooling in February, and by March much of the continent, except the coastal fringe, is approaching zero again, where temperatures remain through the months of darkness, until October. The Antarctic Peninsula, to the north of the main continental mass, has regular frosts in April and May then near-zero temperatures till August. There are still some late frosts in October, but temperatures rise, through 12 °C in November, achieving 16 °C+ in December and January, before declining through February and the onset of early frosts in March.

5.2. Precipitation (Figs. 5C,D and 6A) and climate zones (Fig. 6B)

Because of the high sea surface temperatures, there is a greatly enhanced hydrological cycle, by comparison with the present (Figs. 5 and 6). Much convective rainfall is over the equatorial regions and particularly over the oceans.

During JJA, the zone of highest rainfall, and where precipitation far exceeds evaporation, lies just N of equator under the ITCZ. Most of northwest Africa has an excess of precipitation (P>E), implying the potential for deep weathering and major seasonal run-off. The northern part of Africa is modelled to have strongly seasonal humidity, drying during DJF. Late Cretaceous coals and kaolinite typify the area modelled to have nearly year-round moisture, whereas evaporites and calcretes are recorded from the more arid areas in the north (Scotese 2000).

On the northern margins of European Tethys, the scattered landmasses receive significant precipitation during the summer season (summerwet, biome 2 being most likely). Tethys itself and the eastern lands of Iran through China have an excess of evaporation, although northern China and Japan have an increase in moisture during the summer (summerwet, possible biome 2). Southern and central parts of China are modelled to be mostly dry (desert) with semi-arid steppes extending northwards across Mongolia and northeastern Siberia. Westwards across Eurasia moister conditions ensued (winterwet) with the potential for extensive forests over Scandinavia and Central Europe.

Most northern latitude land areas are close to balance with respect to evaporation and precipitation, although high lands to the west of the Midwest Seaway in North America have a modest excess of moisture in summer and a significant excess during the winter, offering the potential for deep weathering, major run-off and peat/coal formation, as is confirmed by facies distributions in Scotese (2000).

In the southern hemisphere, a broad zone with excessive evaporation extends from the equator to beyond 30°S, embracing the central parts of South America and Central Africa.

Most of northern South America remains dry from July to October (seasonally wet–dry). However, the most northwestern part of South America is wet year-round, producing the potential for a tropical humid area (biome 1). Argentina and Chile, at around palaeolatitude

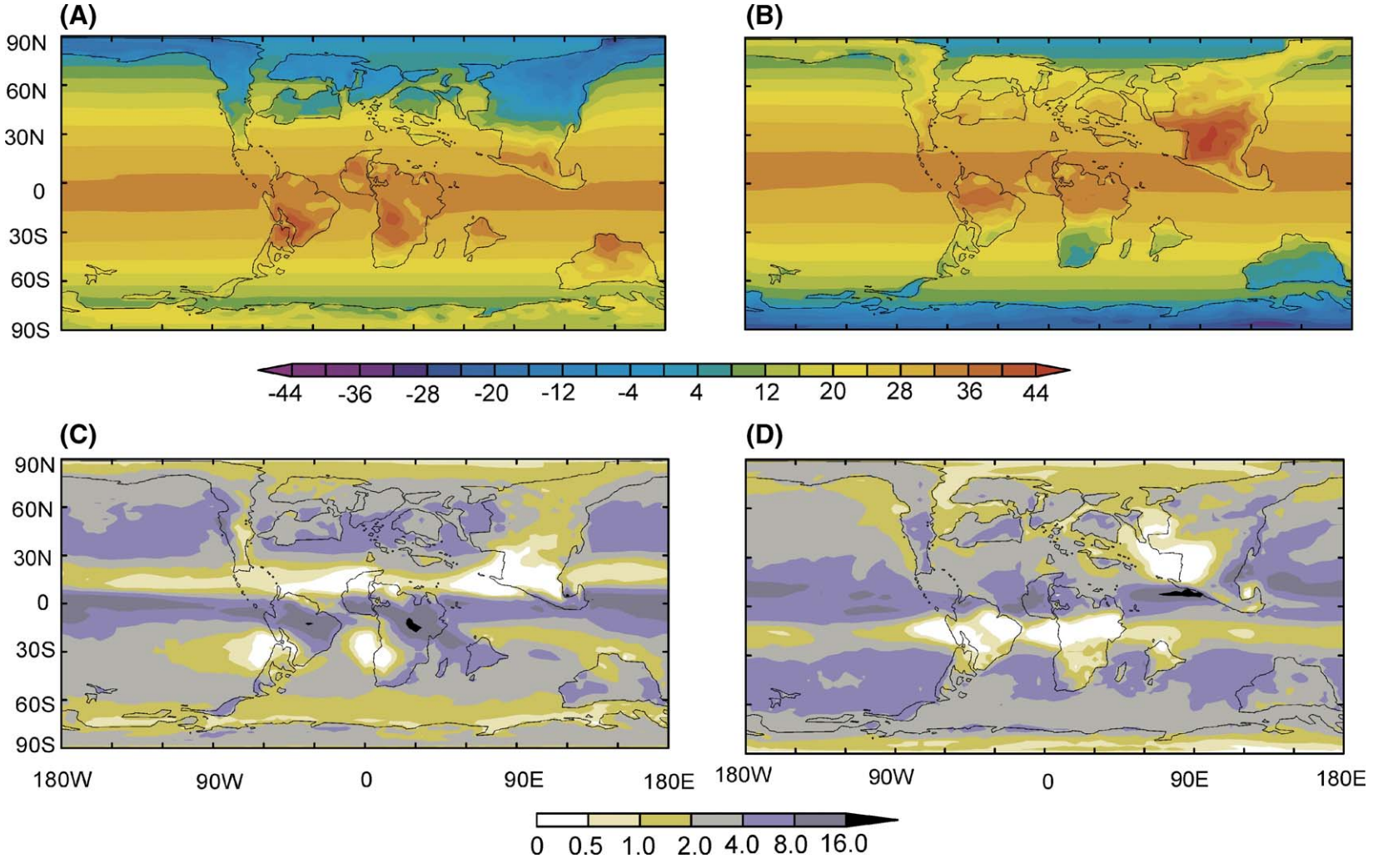

Fig. 5. (A and B) Model simulated, mean seasonal temperatures for the Late Cretaceous for (A) December–January–February season and (B) June–July–August season. Units are in °C and the contour interval is every 4 °C. (C and D) Model simulated, mean seasonal precipitation for the Late Cretaceous (C) December–January–February season and (D) June–July–August season. Units are in mm/day and the contour interval is not regular.

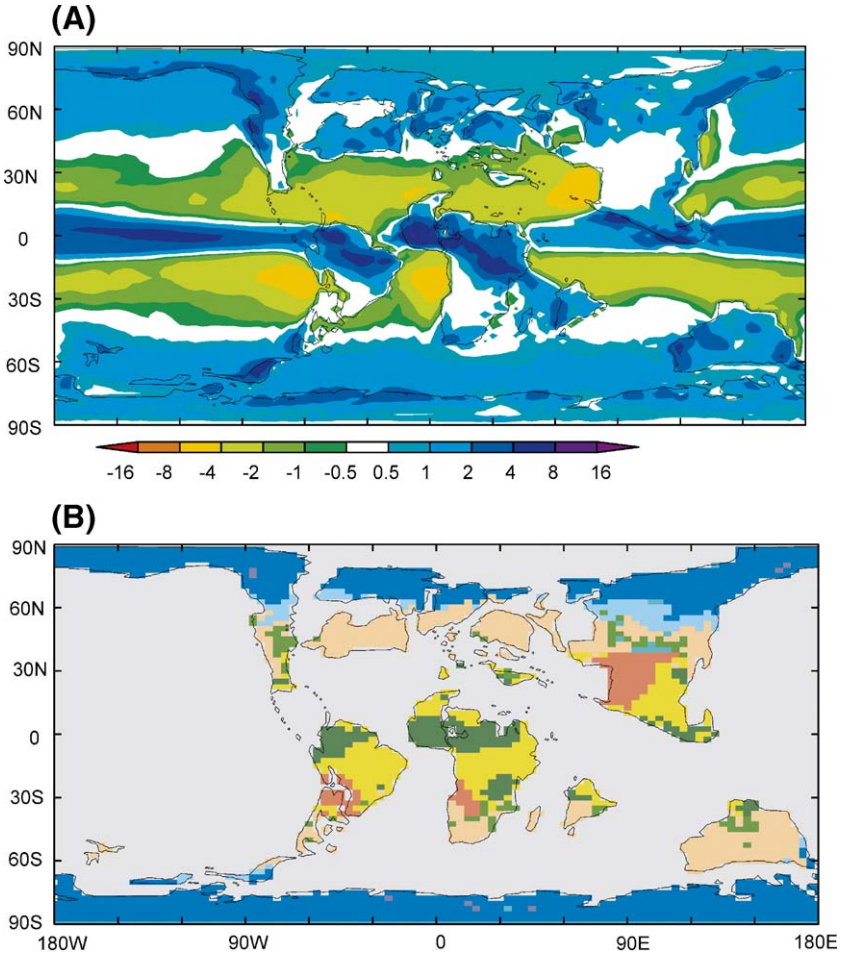

Fig. 6. (A) Modelled precipitation minus evaporation in mm/day for the Late Cretaceous (negative values indicate excess evaporation over precipitation). (B) The Walter biome zones for the Late Cretaceous based on the model predicted temperatures and precipitation. Key to zones as in Fig. 2C.

30°S, was an area predominantly dry year-round, with a short wet season in February (summerwet) but, being predominantly dry, a tropical xerophytic/desert, biome 3, would be expected. Generally moister conditions exist year-round south of 40°S and would have allowed the development of warm mixed forests (biome 5) and temperate coniferous forests (biome 6) over southern Patagonia.

A plume of convective moisture extends across the opening Central Atlantic into W Africa and across large tracts of the present-day Sahara/Sahel. Northwestern Africa was predominantly dry with a June–August wet season (summer wet, biome 2). To the South, the wet season commences over eastern parts of Africa from around October, but high evaporation also occurs here. SW Africa is very dry desert area (biome 3). Southern Africa is moist more-or-less year-round and would have supported temperate deciduous forests and warm mixed forests (biomes 5 and 6).

Southeast Asia was predominantly humid (rainforest) but with a short dry season in August (biomes 1 to 2). India has year-round rain but evaporation exceeds precipitation for much of the year, making xerophytic flora the most likely. Its wettest zone exists in the northeastern area, where evergreen forest could have grown.

During DJF, the northern Polar lands of Greenland, Canada and USA, although receiving less precipitation, have much less evaporation. Significant precipitation both here and in Siberia is as winter snow. Northern mid-latitudes have an excess of winter moisture in a zone extending almost as far south as 30°N. Evaporation predominates from here to just north of the equator, and embracing northern and much of western Africa, which

experiences a dry season. Iran to China remain parched and stay so year-round. The humid zone has moved south with the ITCZ bringing monsoonal rains to large tracts of present-day Brazil, Central Africa and southern Arabia.

Except in its far northern more arid zone Australia is modelled to have had sufficient moisture to be extensively forested, warm in the north and temperate in the south. Antarctica is a dry continent but just about in balance year-round with respect to evaporation and precipitation, with much of the winter precipitation as snow (e.g. in July).

Evaporation and precipitation (coupled with local run-off) have an impact on the salinities of ocean waters. In the open Pacific and Indian Oceans, these are at their most saline at around 30°N and 30°S, with equatorial zones of high salinity too (>36‰), and through the Tethyan belt (Caribbean-C Atlantic-Med-Mid East-Iran). Marine salinities are highest over areas now occupied by Algeria (38–40‰) and Iran (38–45‰). Water salinities are also high in Argentina and Chile embayments. Throughout the Midwest Seaway, salinities are low (approaching 30‰) and remain low into the enclosed Arctic Basin, promoting there the formation locally of winter sea ice.

The simulations shown above were based on a very simple distribution of ocean temperatures. We are currently in the process of performing fully coupled atmosphere–ocean models for the late Cretaceous. Preliminary results suggest that the results shown above are robust and are relatively insensitive to changes to the ocean temperatures. Interestingly, the coupled models are predicting small amounts of seasonal sea ice in both hemispheres. Nonetheless, the high-latitude ocean temperatures increase in summer to 10 °C or more, resulting in above zero mean annual temperatures.

5.3. Output from other models and the geological evidence

According to Poulsen et al. (2001) and Skelton et al. (2003), the mid-Cretaceous was a time of unusually active tectonism and seafloor spreading, associated with enhanced volcanic outgassing. In the marine realm, this is a time of episodic Oceanic Anoxic Events (OAEvent 1—Aptian–Early Albian; OAEvent 2—Cenomanian/Turonian boundary). Outgassing caused enhanced CO_2 levels in the atmosphere, and plate movements caused palaeogeographic changes that caused major global oceanic circulation, in particular the presence or absence of a marine connection between the North and South Atlantic. Reporting model experiments employing the NCAR Parallel Ocean Climate Model, Poulsen et al. (2001) suggest that, during the Turonian, a gateway or sill opened in the Atlantic allowing Antarctic Bottom Water to ventilate the Atlantic basins. Handoh et al. (1999) have modelled paleo-upwelling and organic rich sediments in the Cenomanian Atlantic and confirm that a critical factor controlling North Atlantic ventilation was the establishment, for the first time, of connection between the North and South Atlantic Oceans in the Turonian. A series of global changes in climate and oceanography at the Cenomanian/Turonian boundary were probably triggered by the initiation of this connection between the formerly separated Atlantic Oceans. Beckmann et al. (2005), using ODP data from offshore Ivory Coast (W Africa) and GCM simulations, have argued for precession-driven fluctuations in river discharge during the Coniacian–Campanian. Phases of enhanced outflow can here be linked with episodes of oceanic anoxia.

5.4. Cretaceous vegetation and biomes

Using the GENESIS model to evaluate the coupled climate-vegetation system, applying a predictive vegetation model (EVE), DeConto et al. (2000) simulated climate, vegetation and ocean interactions. Vegetation simulations were justifiably tuned by the elimination of grasses and sedges (which had yet to appear). They found that broadleaf herbaceous angiosperms (referred to as “forbs”), ferns and shrubs dominate the cover in the niche today occupied by grasslands, generating what they term a “forb-fern prairie”. To maintain the types of high-latitude coastal and continental climates warm enough to sustain the plant and animal communities now well documented from very high latitudes in both hemispheres, they needed to run the model with 1680 ppm CO_2 in the atmosphere. Under these simulated conditions, the Antarctic Peninsula became forested by evergreen linear-leaf trees (*Araucaria* and *Podocarpus*), a situation comparable with known fossil occurrences. In the Arctic, boreal forests were fringed by forb-fern prairie. Tropical ocean temperatures are modelled to have reached 30–33 °C, that is warmer than at present and a little warmer than most values calculated by reference to oxygen isotope studies (e.g. Crowley and Zachos, 2000). Although the Equator-to-Pole thermal gradient is much reduced by comparison with present-day values (mean annual equatorial SST of 32 °C and polar seawater value of 8 °C), but despite this the simulation has surface circulations almost as vigorous as those of the present. This ocean heat

transport provides a mechanism for enhancing the warming of coastal zones in high latitudes. The absence of a circum-Antarctic ocean precludes the development of an Antarctic Circum Polar Current. Persistent low pressures over continents generated convergence zones and the advection of warm moist air from the oceans into continental interiors. High-latitude forests maintained a relatively low albedo in these areas and this, coupled with warm summer temperatures helped to maintain polar warmth in a self-perpetuating system. Deep waters within the ocean are simulated to have formed in high southern latitudes with temperatures of 10–12 °C and salinities of around 35‰.

5.5. Temperature-limited facies

Johnson et al. (2002) record the distribution of Cretaceous reefs. Coral and rudistid reefs are generally considered to have been warm-water facies (Beauvais, 1992), rudist bioherms being restricted to generally lower latitudes than were coral buildups. Nonetheless, through the Cenomanian to Santonian coral reefs extended to nearly 40°N (in Europe and New Mexico) and to 40°S (Madagascar). The main focus of reef growth at this time was through the Tethyan belt from the Caribbean, through Mediterranean Europe and the Middle East. In the latest Cretaceous, corals are more restricted, ranging from scattered sites along the equator to about 40°N in northern France. Rudist reefs extend from just south of the equator to about 35°N. It is interesting to note that the high salinity/high temperature zones in the model correspond generally with the distribution of rudist-dominated reef communities (cf. Johnson et al., 2002). By reference to cold month means temperatures in our model it is noticeable that the 24 °C isotherm lies much closer to the equator in the southern hemisphere than it does in the northern hemisphere (approaching 20°S and 30°N). It is worth noting that Johnson et al. (2002) show a similarly asymmetric distribution of reef belts.

By reference to facies and other climate proxies the mid-Cretaceous (~105 to ~89 Ma) appears to have been one of the warmest time intervals of the Phanerozoic (Veizer et al., 2000, reviewed in Johnson et al., 2002). Warm and cool temperate climates extended into high polar latitudes (Askin and Spicer, 1995; Herman and Spicer, 1996; Tarduno et al., 1998). Isotopic data from planktic foraminifera suggest SSTs as high as 35 °C (Norris et al., 2002; Wilson et al., 2002) and high-latitude SSTs at 20 °C or above (Huber et al., 1995; Bice et al., 2003). Bottom water temperatures, derived from benthic foraminifera, suggest that palaeodepths greater that 1 km ranged between 11 °C and 19 °C (Huber et al., 1999, 2002).

Estimates of atmospheric CO_2 concentrations range widely between <900 ppm and >4000 ppm, being derived from fossil leaf stomal indices. Ginkgo species in Siberia suggest values between 4000 and 5500 ppm (Retallack, 2001). However, C isotopic values derived from marine organic compounds from the Western Interior Seaway of N America and North Atlantic have been interpreted to indicate values as low as 830–1100 ppm (Freeman and Hayes, 1992). A wide range of other values have also been obtained based on analyses of fossil pedogenic carbonates (e.g. Cerling, 1991, who estimates 1500–3000 ppm). Berner and Kothavala (2001) suggest values of around 1500 ppm at the start of the Cretaceous, falling gradually towards 1000 ppm by the mid-Campanian and then dropping towards ~800 ppm approaching the K–T boundary. Ekart et al. (1999) suggest a similar trend in values but a much broader range (from >2500 ppm at the start of the Cretaceous declining to around 500 ppm at its close). All these authors indicate a wide measure of uncertainty, which typifies such evaluations, with many researchers listing error bars exceeding 1500 ppm. Nonetheless, as Bice and Norris (2002) point out, to have SSTs in tropical and temperate latitudes as high as 30 °C may require CO_2 concentrations as high as 4500 ppm or more. They furthermore speculate that the CO_2 content of the atmosphere may have been highly dynamic, exhibiting wide fluctuations and over a variety of time scales.

Saltzman and Barron (1982) reported evidence of saline deep water masses within the Campanian/Maastrichtian South Atlantic, based on the $\delta^{18}O$ values derived from inoceramid shells. Such data have been refined more recently and D'Hondt and Arthur (2002) are now able to recognise, on the basis of stable isotopic data from benthic foraminifera, at least three deepwater masses in the late Maastrichtian oceans. The coolest intermediate-depth water gives temperatures of ~6 °C and originated in high-latitude Southern Ocean. The deepest waters give 10 °C and probably originated in the northern Atlantic. The warmest intermediate waters were 13–15 °C and have an unknown source. Much of this deep water, they suggest, was preconditioned for winter sinking by low- or middle-latitude evaporation (much as are the Mediterranean, Red Sea, and North Atlantic waters today), but only a small proportion (~10 °C) of it could have come directly from such a source. Thus low- or mid-latitude evaporation is likely to have played a significant role in preconditioning some surface waters for sinking, but the sinking being

actuated by seasonal cooling of such waters. Warm waters would have generally restricted the oceanic storage capacity for both CO_2 and methane hydrates, by comparison with ice house times, such as the present and later Cenozoic.

Based on isotopic data derived from planktic foraminifera, there have been several claims that oceanic equatorial waters were only as warm as, or cooler, during the Cretaceous than at present, despite the general equability indicated by strong evidence of polar warmth (e.g. Sellwood et al., 1994 [~25–26 °C]; D'Hont and Arthur, 1996 [~20–21 °C]). Also using $\delta^{18}O$ values, but from pristine shell material, Wilson and Opdyke (1996) have shown that rudist reefs grew at 27–32 °C (i.e. at least as warm as at present). So the apparently cooler temperatures reported can now be explained by cryptic diagenetic alteration of foraminiferan shells in cool oceanic bottom waters (Pearson et al., 2001) with equatorial values of 28–32 °C being confirmed. Jenkyns et al. (2004) have recently interpreted Maastrichtian Arctic marine palaeotemperatures using TEX_{86}, a palaeothermometer based on the membrane lipids from marine planktonic Crenarchaeota. They inferred SSTs of ~15 °C at 80°N (Alpha Ridge, Arctic Ocean) but this probably reflects summer temperatures and that mean annual temperatures are much lower, with the possibility of seasonal sea ice. This value, when compared with the equatorial temperatures cited above, gives an equator to north pole gradient of a mere 15 °C. Huber et al. (1995) had previously inferred an equator to South pole gradient of ~14 °C based on oxygen-isotopic ratios from planktonic foraminifera. Nonetheless, there appears to be a well documented trend towards cooler global oceanic temperatures, and cooler and less saline bottom waters, approaching the end of the Cretaceous (reviewed in MacLeod and Huber, 2000).

By reference to the palaeo-distribution of fossil crocodilians, Markwick (1998) has evaluated the cooling in Earth's climate over the past 100 Ma. He shows that temperature is the principal influence on crocodilian global distributions, with the coldest month mean temperature (CMM) of 5.5 °C marking the minimum thermal limit for the group (corresponding to a modern mean annual temperature (MAT) of ~14.2 °C). He suggests that during the late Cretaceous and early Palaeogene MATs in excess of 14.4 °C (CMMs > 5.5 °C) permeated throughout mid-latitudes and coastal regions in high latitudes. Crocodiles are recorded just N of 30°N in N America and 43°S in S America, in the latter case associated with turtles. Turtles are also recorded from India at 35°S. Crocodiles extend to 40°N in China and 30°N in Europe. These distributions are close to a modelled CMM of 6 °C in China, >8 °C in Europe and >8 °C in Patagonia. But they occur in areas modelled to have a CMM of −8 °C in North America, clearly presenting a major discrepancy between model output and geological reality. The remarkable fossil evidence that several groups of dinosaurs were feather-insulated (e.g. in China) is quite compatible with the low winter temperatures modelled in these areas. If modelled temperatures are correct, then many dinosaur groups living in mid- to high latitudes are likely to have been feathered.

6. Conclusions

Model simulations for the Mesozoic throw important light on climatic processes, and the behaviour of Earth Systems, under greenhouse conditions. The model output generally compares favourably with climate proxy data, but discrepancies between data and models reveal some serious modelling problems (or possibly incorrect interpretation of the proxies). In continental interiors, model simulations generate winter conditions considered to be too cold (by 15 °C or more) by reference to palaeontological data.

Ocean temperatures could have been much warmer than today, not only at the surface but also to great depths (8 °C to the ocean floor). Such temperatures would have greatly reduced the oceanic storage capacity both for CO_2 (in ocean waters) and methane hydrates (in ocean-floor sediments) by comparison with the present day. The simulations shown in this paper are with atmosphere only models which require the specification of surface ocean conditions. However, we based these sea surface temperatures on preliminary results from fully coupled model simulations for these periods. Thus, the close agreement between model output and proxy climate data in coastal and open sea areas suggests that the models are performing well.

In its greenhouse mode, the Earth has greatly enhanced evaporation and precipitation, by comparison with the present, but much of the rainfall is convective in character, falling over the oceans. To replicate climatic conditions similar to those indicated by proxy facies, a very large increase in atmospheric CO_2 is required (at least 4 × present-day values).

References

Allen, JRL, Hoskins, B.J., Sellwood, B.W., Spicer, R.S., Valdes, P.J. (Eds.), 1994. Palaeoclimates and their Modelling: With Special Reference to the Mesozoic Era. Chapman and Hall. 140 pp.

Arkell, W.J., 1956. Jurassic Geology of the World. Oliver and Boyd, Edinburgh.

Askin, R.A., Spicer, R.A., 1995. The late Cretaceous and Cenozoic history of vegetation and climate of northern and southern high latitudes: a comparison. Effects of Past Global Change on Life. Studies in Geophysics, National Research Council. National Academy Press, Washington, pp. 156–173.

Barron, E.J., 1983. A warm equable Cretaceous: the nature of the problem. Earth-Science Reviews 19, 305–338.

Barron, E.J., 1987. Eocene equator-to-pole surface ocean temperatures: a significant climate problem. Palaeogeography, Palaeoclimatology, Palaeoecology 2, 729–740.

Barron, E.J., Washington, W.M., 1985. Warm Cretaceous climates: high atmospheric CO_2 as a plausible mechanism. In: Sundquist, E.T., Broeker, W.S. (Eds.), The Carbon Cycle and Atmospheric CO_2: Natural Variations Archean to Present. Geophys. Monogr. Series. AGU, Washington, DC, pp. 546–553.

Barron, E.J, Fawcett, P.J., Pollard, D., Thompson, S., 1994. Model simulations of Cretaceous climates: the role of geography and carbon dioxide. In: Allen, J.R.L., Hoskins, B.J., Sellwood, B.W., Spicer, R.S., Valdes, P.J. (Eds.), Palaeoclimates and their Modelling: With Special Reference to the Mesozoic Era. Chapman and Hall, pp. 99–108.

Beauvais, L., 1992. Palaeobiogeography of the early Cretaceous corals. Palaeogeography, Palaeoclimatology, Palaeoecology 92, 233–247.

Beckmann, B., Flogel, S., Hofmann, P., Schulz, M., Wagner, T., 2005. Orbital forcing of Cretaceous river discharge in tropical Africa and ocean response. Nature 437, 241–244.

Benton, M.J., 2003. When Life Almost Died. Thames and Hudson Ltd, London. 336 pp.

Berner, R.A., Kothavala, Z., 2001. GEOCARB III: a revised model of atmospheric CO_2 over Phanerozoic time. American Journal of Science 301, 182–204.

Bice, K.L., Norris, R.D., 2002. Possible atmospheric extremes of the Middle Cretaceous (Albian-Turonian). Paleoceanography 17 (4), 1070. doi: 10.1029/2002PA000778, 202.

Bice, K.L., Huber, B.T., Norris, R., 2003. Extreme polar warmth during the Cretaceous greenhouse? Paradox of late Turonian ^{18}O record at Deep Sea Drilling Project Site 511. Paleoceanography 18 (2), 1031. doi:10.1029/2002PA000848.

Billups, K., Schrag, D.P., 2002. Paleotemperatures and ice volume of the past 27 Myr revisited with paired Mg/Ca and $^{18}O/^{16}O$ measurements from benthic foraminifera. Paleoceanography 17 (1), 3-1–3-11.

Bjerrum, C., Surlyk, F., Callomon, J.H., Slingerland, R.L., 2001. Numerical paleoceanographic study of the early Jurassic transcontinental Laurasian Seaway. Paleoceanography 16, 390–404.

Chandler, M.A., Rind, D., Ruedy, R., 1992. Pangaean climate during the early Jurassic: GCM simulations and the sedimentary record of palaeoclimate. Geological Society of America Bulletin 104, 543–559.

Cerling, T.E., 1991. Carbon dioxide in the atmosphere: evidence from Cenozoic and Mesozoic paleosols. American Journal of Science 291, 377–400.

Crowley, T.J., 1996. Remembrance of things past: greenhouse lessons from the geological record, Consequences, 2, U.S. GCRIO [Online] (Available at http://www.gcrio.org/CONSEQUENCES/winter96/geoclimate.html).

Crowley, T.J., North, G.R., 1991. Paleoclimatology. Oxford University Press. 349 pp.

Crowley, T.J., Zachos, J.C., 2000. Comparison of zonal temperature profiles for past warm time periods. In: Huber, B.T., MacLeod, K.G., Wing, S.T. (Eds.), Warm Climates in Earth History. Cambridge University Press, pp. 50–76.

DeConto, R.M., Brady, E.C., Bergengren, J., Hay, W.W., 2000. Late Cretaceous climate, vegetation and ocean interactions. In: Huber, B.T., MacLeod, K.G., Wing, S.T. (Eds.), Warm Climates in Earth History. Cambridge University Press, pp. 275–296.

D'Hont, S., Arthur, M.A., 1996. Late Cretaceous oceans and the cool tropic paradox. Science 271, 1838–1841.

D'Hondt, S., Arthur, M.A., 2002. Deep water in the late Maastrichtian ocean. Paleoceanography 17 (1). doi:10.1029/1999PA000486.

Ekart, D.D., Cerling, T.E., Montanex, I.P., Tabor, N.J., 1999. A 400 million year carbon isotope record of pedogenic carbonate: implications for paleoatmospheric carbon dioxide. American Journal of Science 299, 805–827.

Flügel, E., 2002. Triassic reef patterns. In: Kiessling, W., Flügel, E., Golonka, J. (Eds.), Phanerozoic Reef Patterns. SEPM Special Publication, vol. 72. Tulsa, pp. 391–463.

Frakes, L.A., 1979. Climates Throughout Geologic Time. Elsevier, Amsterdam. 310 pp.

Frakes, L.A, Francis, J.E., Syktus, J.I., 1992. Climate Modes of the Phanerozoic. Cambridge. 274 pp.

Freeman, K.H., Hayes, J.M., 1992. Fractionation of carbon isotopes by phytoplankton and estimates of ancient CO_2 levels. Global Bigeochemical Cycles 6 (2), 185–198.

Hall, I.R., McCave, I.N., Zahn, R., Carter, L., Knutz, P.C., Weedon, G.P., 2003. Paleoceanography 18 (2), 1040. doi:10.1029/2002PA000817.

Hallam, A., 1975. Jurassic Environments. Cambridge University Press. 269 pp.

Hallam, A., 1985. A review of Mesozoic climates. Journal of the Geological Society (London) 142, 433–445 (Change to 1985 in text).

Hallam, A., 1994. Jurassic climates as inferred from the sedimentary and fossil record. In: Allen, J.R.L., Hoskins, B.J., Sellwood, B.W., Spicer, R.S., Valdes, P.J. (Eds.), Palaeoclimates and their Modelling: With Special Reference to the Mesozoic Era. Chapman and Hall, pp. 79–88.

Handoh, I.C., Bigg, G.R., Jones, E.J.W., Masamichi, I., 1999. An ocean modelling study of the Cenomanian Atlantic: equatorial paleo-upwelling, organic-rich sediments and the consequences for a connection between the proto-North and South Atlantic. Geophysical Research Letters 26, 223–226.

Haywood, A.M., Valdes, P.J., Sellwood, B.W., Kaplan, J.O., 2002. Antarctic climate during the middle Pliocene: model sensitivity to ice sheet variation. Palaeogeography, Palaeoclimatology, Palaeoecology 182, 93–115.

Herman, A.B., Spicer, R.A., 1996. Palaeobotanical evidence for a warm Cretaceous Arctic Ocean. Nature 380, 330–333.

Huber, B.T., Watkins, D.K., 1992. Biogeography of Campanian–Maastrichtian calcareous plankton in the region of the Southern Ocean: paleogeographic and palaeoclimatic implications. In: Kennett, J.P., Warnke, D.A. (Eds.), The Antarctic Paleoenvironment: A Perspective on Global Change: American Geophysical Union, Antarctic Research Series, vol. 56, pp. 31–60.

Huber, B.T., Hodell, D.A., Hamilton, C.P., 1995. Mid- to Late Cretaceous climate of the southern high latitudes: stable isotopic evidence for minimal equator-to-pole thermal gradients. Geological Society of America Bulletin 107, 1164–1191.

Huber, B.T., Leckie, R.M., Norris, R.D., Bralower, T.J., CoBabe, 1999. Foraminiferal assemblage and stable isotopic change across the Cenomanian–Turonian boundary in the subtropical North Atlantic. Journal of Foraminiferal Research 29, 392–417.

Huber, B.T., MacLeod, K.G., Wing, S.T. (Eds.), 2000. Warm Climates in Earth History. Cambridge University Press. 462 pp.

Huber, B.T., Norris, R.D, MacLeod, K.G., 2002. Deep-sea paleotemperature record of extreme warmth during the Cretaceous. Geology 30, 123–126.

Jenkyns, H.C., Foster, A., Schouten, S., Damste, J.S.S., 2004. High temperatures in the Late Cretaceous Arctic Ocean. Nature 432, 888–892.

Johnson, C.C., Sanders, D., Kauffman, E.G., Hay, W., 2002. Patterns and processes influencing Upper Cretaceous reefs. In: Kiessling, W., Flügel, E., Golonka, J. (Eds.), Phanerozoic Reef Patterns. In: SEPM Special Publication, vol. 72. Society of Sedimentary Geology, Tulsa, pp. 549–585.

Kutzbach, J.E., Gallimore, R.G., 1989. Pangean climates—megamonsoons of the megacontinent. Journal of Geophysical Research [Atmospheres] 94 (D3), 3341–3357.

Kutzbach, J.E., Ziegler, A.M., 1994. Simulation of late Permian climate and biomes with an atmosphere–ocean model—comparisons with observations. Philosophical Transactions of the Royal Society of London. Series B 341, 327–340.

MacLeod, K.G., Huber, B.T., Ducharme, M.L., 2000. Paleontological and geochemical constraints on the deep oceans during the Cretaceous greenhouse interval. In: Huber, B.T., MacLeod, K.G., Wing, S.T. (Eds.), Warm Climates in Earth History. Cambridge University Press, pp. 241–274.

Markwick, P.J., 1998. Fossil crocodilians as indicators of late Cretaceous and Cenozoic climates: implications for using palaeontological data in reconstructing palaeoclimate. Palaeogeography, Palaeoclimatology, Palaeoecology 137, 205–271.

Meyen, S.V., 1997. Permian conifers of western Angaraland. Review of Palaeobotany and Palynology 96, 351–447.

Moore, G.T., Hayashida, D.N., Ross, C.A., Jacobson, S.R., 1992a. Paleoclimate of the Kimmeridgian/Tithonian (late Jurassic) world: I. Results using a general-circulation model. Palaeogeography, Palaeoclimatology, Palaeoecology 93, 113–150.

Moore, G.T., Sloan, L.C., Hayashida, D.N., Ross, C.A., Umrigar, N.P., 1992b. Paleoclimate of the Kimmeridgian/Tithonian (late Jurassic) world: II. Sensitivity tests comparing 3 different paleotopographic settings. Palaeogeography, Palaeoclimatology, Palaeoecology 95, 229–252.

Norris, R.D., Bice, K.L., Magno, E.A., Wilson, P.A., 2002. Jiggling the tropical thermostat in the Cretaceous hothouse. Geology 30, 299–302.

Pearson, P.N., Ditchfield, P.W., Singano, J., Harcourt-Brown, K.G., Nicholas, C.J., Olsson, R.K., Shackleton, N.J., Hall, M.A., 2001. Warm tropical sea surface temperatures in the late Cretaceous and Eocene epochs. Nature 413, 481–487.

Pope, V.D., Gallani, M.L., Rowntree, P.R., Stratton, R.A., 2000. The impact of new physical parametrizations in the Hadley Centre climate model: HadAM3. Climate Dynamics 16, 123–146.

Poulsen, C.J., Barron, E.J, Arthur, M.A., Peterson, W.H., 2001. Response of the mid-Cretaceous global oceanic circulation to tectonic and CO_2 forcings. Paleoceanography 16, 576–592.

Price, G.D., Sellwood, B.W., 1997. "Warm" palaeotemperatures from high late Jurassic palaeolatitudes (Falkland Plateau): ecological, environmental or diagenetic controls? Palaeogeography, Palaeoclimatology, Palaeoecology 129, 315–327.

Price, G.D., Sellwood, B.W, Valdes, P.J., 1995. Sedimentological evaluation of general circulation model simulations for the "greenhouse" Earth: Cretaceous and Jurassic case studies. Sedimentary Geology 100, 159–180.

Price, G.D., Valdes, P.J., Sellwood, B.W., 1997. Quantitative palaeoclimate GCM validation: late Jurassic and mid-Cretaceous case studies. Journal of the Geological Society (London) 154, 769–772.

Rees, P.M., Zeigler, A.M., Valdes, P.J., 2000. Jurassic phytogeography and climates: new data and model comparisons. In: Huber, B.T., MacLeod, K.G., Wing, S.T. (Eds.), Warm Climates in Earth History. Cambridge University Press, pp. 297–318.

Retallack, G.J., 2001. A 300 million-year record of atmospheric carbon dioxide from fossil plant cuticles. Nature 411, 287–290.

Saltzman, E.S, Barron, E.J., 1982. Deep circulation in the late Cretaceous—oxygen isotope paleotemperatures from *Inoceramus* remains in DSDP cores. Palaeogeography, Palaeoclimatology, Palaeoecology 40, 167–181.

Scotese, C.R., 2000. Paleomap Project, http://www.scotese.com.

Sellwood, B.W., Price, G.D., Valdes, P.J., 1994. Cooler estimates of Cretaceous temperatures. Nature 370, 453–455.

Shackleton, N.J., Kennett, J.P., 1975. Paleotemperature history of the Cenozoic and the initiation of Antarctic glaciation—oxygen and carbon isotope analyses in DSDP Sites 277, 279, and 281. In: Kennett, J.P, Houz, R.E. (Eds.), Initial Reports of the Deep Sea Drilling Project, vol. 29. US Government Printing Office, Washington, DC, pp. 743–755.

Skelton, P., Spicer, R.A., Kelley, S.P., Gillmour, I. 2003. The Cretaceous World. The Open University, Cambridge University Press. 360 pp.

Tarduno, J.A., Brinkman, D.B., Renne, P.R., Cottrell, R.D., Scher, H., Castillo, P., 1998. Evidence for extreme climatic warmth from late Cretaceous Arctic vertebrates. Science 282, 2241–2244.

Taylor, E.L., Taylor, T.N., 2000. In: Huber, B.T., MacLeod, K.G., Wing, S.T. (Eds.), Warm Climates in Earth History. Cambridge University Press, pp. 321–350.

Tripati, A., Backman, J., Elderfield, H., Ferretti, P., 2005. Eocene bipolar glaciation associated with global carbon cycle changes. Nature 436, 341–346.

Tucker, M.E., Benton, M.J., 1984. Triassic environments, climates and reptile evolution. Palaeogeography, Palaeoclimatology, Palaeoecology 40, 361–379.

Valdes, P.J., Sellwood, B.W., 1992. A palaeoclimate model for the Kimmeridgian. Palaeogeography, Palaeoclimatology, Palaeoecology 95, 47–72.

Valdes, P.J., Sellwood, B.W., Price, G.D., 1995. Modelling late Jurassic Milankovitch climate variations. In: House, M.R., Gale, A.S. (Eds.), Orbital Forcing Timescales and Cyclostratigraphy: Geological Society Special Publ., vol. 85, pp. 115–132.

Valdes, P.J., Sellwood, B.W., Price, G.D., 1996. Evaluating concepts of Cretaceous equability. Palaeoclimates 1 (2), 139–158 (Change in text).

Valdes, P.J., Spicer, R.A., Sellwood, B.W., Palmer, D.C., 1999. Understanding Past Climates: Modelling Ancient Weather. Routledge. CD-ROM.

Veizer, J., Godderis, Y., Francois, L.M., 2000. Evidence for decoupling of atmospheric CO_2 and global climate during the Phanerozoic eon. Nature 408, 698–701.

Walter, H., 1985. Vegetation of the Earth. Springer-Verlag, Berlin. 318 pp.

Wilson, P.A., Opdyke, B.N., 1996. Equatorial sea-surface temperatures for the Maastrichtian revealed through remarkable preservation of metastable carbonate. Geology 24, 555–558.

Wilson, P.A., Norris, R.D., Cooper, M.J., 2002. Testing the Cretaceous greenhouse hypothesis using glassy foraminiferal calcite from the

core of the Turonian tropics on Demerara Rise. Geology 30, 607–610.

Zachos, J.C., Breza, J.R., Wise, S.W., 1992. Early Oligocene ice-sheet expansion on Antarctica—stable isotope and sedimentological evidence from Kerguelan Plateau, southern Indian Ocean. Geology 20, 569–573.

Zachos, J.C., Arthur, M.A., Braelower, T.J., Spero, H.J., 2002. Palaeoclimatology—tropical temperatures in greenhouse episodes. Nature 419, 897–898.

Ziegler, A.M., Hulver, M.L., Lottes, A.L., Schmactenberg, W.F., 1984. Uniformitarianism and palaeoclimates: inferences from the distribution of carbonate rocks. In: Brenchley, P.J. (Ed.), Fossils and Climate. Wiley, Chichester, pp. 3–25.

Ziegler, A.M., Parrish, J.M., Jiping, Y., Gyllenhaal, E.D., Rowley, D.B., Parrish, J.T., Shangyou, N., Behher, A., Hulver, M.L., 1994. Early Mesozoic phytogeography and climate. In: Allen, J. R.L., Hoskins, B.J., Sellwood, B.W., Spicer, R.S., Valdes, P.J. (Eds.), Palaeoclimates and their Modelling: With Special Reference to the Mesozoic Era. Chapman and Hall, pp. 89–97.